



## DESIGN AND TESTING OF INERTIA DYNAMOMETER FOR PROTOTYPE FUEL CELL ELECTRIC VEHICLE

Mohd Hadi Anuar Mohd Fakharuzi<sup>1</sup>, Syed Mohd Harussani Syed Omar<sup>1</sup>, Thomas Arthur Ward<sup>2</sup>, Ow Chee Sheng<sup>1</sup>, Suhadiyana Hanapi<sup>1</sup> and Khairul Imran Sainan<sup>1</sup>

<sup>1</sup>Faculty of Mechanical Engineering, MARA University of Technology (UiTM), Shah Alam, Selangor, Malaysia

<sup>2</sup>Department of Mechanical Engineering, Faculty of Engineering Building, University of Malaya, Kuala Lumpur, Malaysia

E-Mail: [fettarnes@hotmail.com](mailto:fettarnes@hotmail.com)

### ABSTRACT

This paper describes and demonstrates the construction and the validation of a customized inertia dynamometer particularly designed for the UiTM urban fuel cell electric vehicle. The inertia dynamometer is designed to simulate real values of vehicle kinetic energy, acceleration resistance, rolling resistance and aerodynamic drag. Parameters used for calibration are taken from the actual road testing and calculated results. This dynamometer is equipped with two data loggers that are able to log voltage, current, speed and time which complement with graphic user interface software for calculating torque and power. As final results, efficiency and energy consumption of the power train system can be calculated and analyzed.

**Keywords:** inertia dynamometer, fuel cell electric vehicle, direct current (DC) motor, data logger, dynamometer calibration.

### INTRODUCTION

Fuel cell electric vehicles (FCEV) have the potential to significantly reduce dependency on crude oil and lower harmful emissions that contribute to climate change [1-6]. FCEV run on hydrogen gas rather than gasoline and emit zero harmful tailpipe emissions. FCEV is a type of electric vehicle which uses a Proton Exchange Membrane (PEM) fuel cell as its source of power supply that produces electricity by an electrochemical reaction process which consumes hydrogen and oxygen while producing electricity and water as a by-product. Hyundai made a step forward when they announced they to be the first car manufacturer to commercialize FCEV in 2012. They have already supplied 100 units of FCEV to be used as taxis in South Korea [7]. This action was followed by the world's largest carmaker Toyota Motor Corporation [8]. Due to the world demand for this technology, it is necessary for Malaysians to learn FCEV technology. One event that promotes FCEV technology is the Shell Eco-marathon Asia competition. In this competition, participants are required to design and build energy efficient cars and finish the race in a given time. The winner is the car that uses the least amount of energy. This competition is an ideal platform as proof of concept to students and researchers who study fuel cell vehicles. UiTM built a single seated prototype-scale vehicle for the Shell Eco-marathon Asia competition. Therefore, the design of the prototype must meet the specifications of the competition where the objective is to finish the race (within the time prescribed) with the most efficient use of energy. To achieve this objective, the vehicle was designed with energy-saving features in every aspect, comprising lightweight, low air resistance, low rolling resistance and a high efficiency power train design. This paper will introduce the methodology of an experimental test bench development. The inertia dynamometer designed was constructed specifically for the UiTM prototype FCEV.

### METHODOLOGY

#### Vehicle acceleration mathematical modelling

Understanding vehicle acceleration is a key in designing a proper dynamometer. During acceleration, there are some forces acting on the vehicle. This force is equivalent to the force required to propel the vehicle forward. They are known as total tractive effort,  $F_{te}$  which consists of: rolling resistance force,  $F_{rr}$ , aerodynamic force,  $F_{ad}$ , hill climbing force,  $F_{hc}$ , linear acceleration force,  $F_{la}$  and the force required to give angular acceleration to the rotating motor,  $F_{\omega a}$ .

$$F_{te} = F_{rr} + F_{ad} + F_{hc} + F_{la} + F_{\omega a} \quad (1)$$

The elements of all forces without accounted for the hill climbing force are equivalent to:

$$\frac{G}{r} \eta T = \mu_{rr} m g + 0.625 A C_d v^2 + (m + \frac{IG^2}{\eta_G r^2}) \frac{dv}{dt} \quad (2)$$

where  $G$  is a gear ratio,  $r$  for wheel radius,  $\mu_{rr}$  is rolling coefficient,  $A$  is vehicle frontal area,  $C_d$  is drag coefficient,  $m$  is vehicle mass,  $(IG^2)/(\eta_G r^2)$  is an angular acceleration mass factor normally determined by 5% from vehicle mass [9],  $\eta$  for gear efficiency,  $dv/dt$  is for acceleration, and  $T$  is equal to torque. These parameters are listed in Table-1. A picture of the vehicle is shown in Figure-1.



Figure-1. UiTM third generation urban fuel cell car named Bat-Motive.

In order to model vehicle acceleration, the DC motor torque must be calculated. Torque is directly proportional to the current. The relationship between torque and current are shown in Equation (3), Equation (4) and Equation (5) where  $I$  is an armature current,  $V_s$  is a terminal voltage,  $R_a$  is an armature resistance,  $K_m$  is a torque constant, and  $\omega$  is a motor speed while  $T_f$  is a torque friction. The consideration of a torque friction in torque equation will present more modeling accuracy [10]. Table-2 shows motor parameters given by the manufacturer. However, for more accurate modeling results, no load current and no load speed value must be taken from the actual test.

Table-1. Vehicle parameters.

Vehicle dynamic parameters	values	Vehicle dynamic parameters	values
Vehicle mass + driver, $m$ (kg)	170	Drag reference area, $A$ (m <sup>2</sup> )	0.93
Angular acceleration mass factor, $(\frac{I_G^2}{I_G^2})$ (kg)	8.5	Coefficient of drag, $C_d$	0.27
Rolling resistance coefficient, $\mu_{rr}$	0.015	Wheel radius, $r$ (m)	0.27

$$I = \frac{V_s}{R_a} - \frac{K_m}{R_a} \omega \tag{3}$$

$$T = IK_m - T_f \tag{4}$$

$$T - (\frac{V_s}{R_a} - \frac{K_m}{R_a} \omega)K_m - T_f \tag{5}$$

$$\frac{v_{n+1} - v_n}{\Delta t} = 0.4228 - 0.0009v^2 \tag{7}$$

$$v_{n+1} - v_n = v_n + \Delta t(0.4228 - 0.0009v^2) \tag{8}$$

This equation holds until the torque begins to fall when,  $\omega = \omega_c$  where  $\omega_c$  stand for critical angular velocity of specific current (in this case 30Amps). After this point, the torque is governed by substitute Equation (5) into Equation (2).

$$\frac{dv}{dt} = 2.28365 - 0.2573v - 0.00089v^2 \tag{9}$$

$$\frac{v_{n+1} - v_n}{\Delta t} = 0.4228 - 0.0009v^2 \tag{10}$$

$$v_{n+1} - v_n = v_n + \Delta t(0.4228 - 0.0009v^2) \tag{11}$$

Table-2. DC motor parameters.

DC motor parameters	Values
Motor constant, $K_m$ (Nm/A)	0.1624
Supply voltage, $V_s$ (V)	36
Armature resistance, $R_a$ ( $\Omega$ )	0.24
No load speed, $N_0$ (RPM)	2120
No load current, $I_0$ (A)	0.61

The vehicle acceleration was performed with maximum power available from fuel cell which is 30 A. The testing must be done with a constant voltage supply to simplify the analysis and comparison. In this case, 36 V is the best voltage to use because of the available fuel cell voltage is 33 V to 48 V.

For example of 30 A, the mathematical modeling of vehicle acceleration is governed by substituting Equation (4) into Equation (2) that becomes:

$$\frac{dv}{dt} = 0.4228 - 0.0009v^2 \tag{6}$$

Equation (6) is then rearranged to obtain the value of the next velocity from the current velocity. This is done as Equation (7) and Equation (8):

**Inertial dynamometer design methodology**

An inertia dynamometer is used for dynamic testing. This means when the throttle is opened, the drum always accelerates. They can determine wheel dynamic torque based on (inertia of rotating drum x angular acceleration = torque). An inertia type dynamometer is a very useful tool to provide dynamic profile of torque versus speed [15]. By understand the fundamental of DC motor, we can observe the detailed dynamic profile and the detailed acceleration analysis can be done through this methodology. The relationship between the net external torque and the angular acceleration is in the same form as Newton's second law and is sometimes called Newton's second law for rotation. Equation (12) is the



fundamental of inertial dynamometer development where torque,  $\tau$  is measured by the product of flywheel moment of inertia and recorded flywheel angular acceleration.

$$\tau = I\alpha \tag{12}$$

**Simulating acceleration component**

The idea of making this test bench is based on emulating an actual vehicle load on the test bench. As in the figure, for acceleration resistance, vehicle inertia and wheel inertia was emulated using a combination of shafts, go kart wheel and pieces of iron wheels. These parts are called the flywheel. The design was made in a circular shape as to avoid the effects of wind resistance when spinning the flywheel. Then, the actual vehicle

aerodynamic resistance was emulated using a ‘Ruston turbine’ concept. Ruston turbine design consists of rectangular blades and rotates with the center axis of the flywheel. The blade is oriented normal to the direction of air flow. The use of two blades in the design aims to strike a balance weight on the flywheel so as to avoid vibration during rotation of the flywheel. Next, the actual rolling resistance of the vehicle is emulated using a load placed above the frame that holds the vehicle wheel. Only one wheel was used in the test bench as the actual vehicle also uses a single traction wheel. Figure-2 is shown a illustration of car loads and test bench loads.

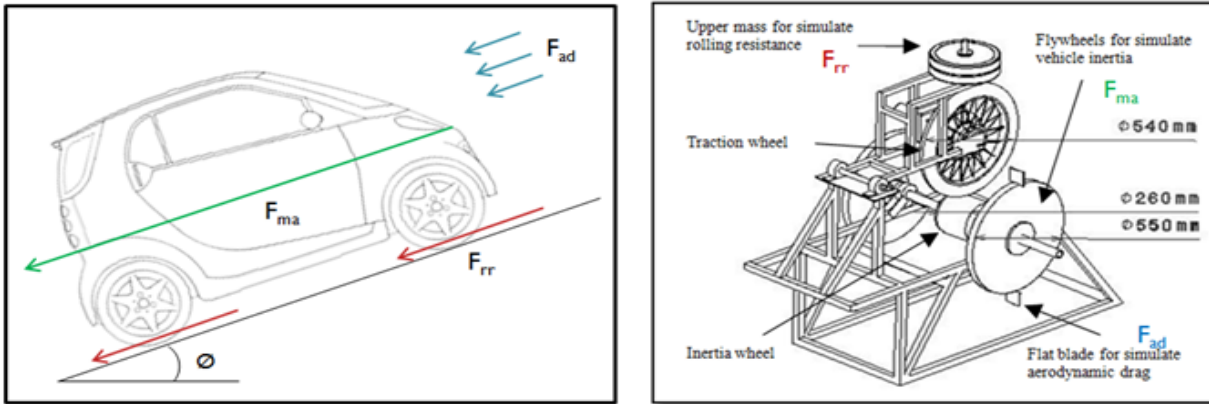


Figure-2. Illustration of car loads and test bench loads.

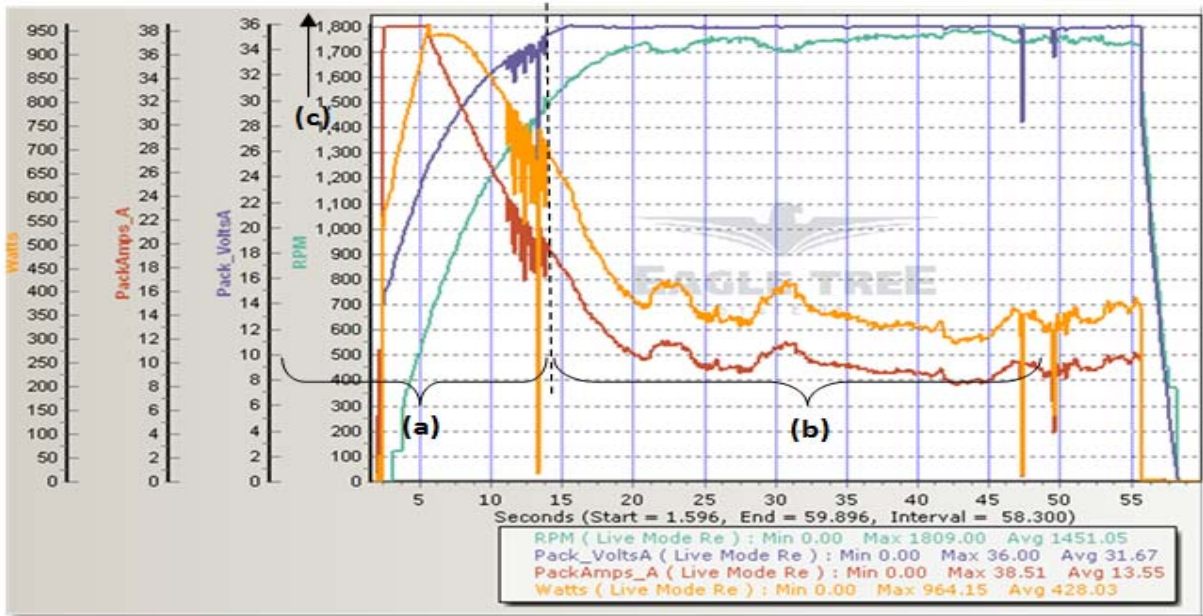


Figure- 3. Data recorded by Eagle Tree data logging system of full acceleration on road car testing, (a) Acceleration time, (b) Constant speed region, (c) Maximum current.



The first step in the designing a test bench is to make an actual road test run. During this test run, data were recorded using the Eagle Tree data logging system. The parameters recorded were voltage, current speed and power input. As in Figure-3, the observation can be made by looking at the curves profile. The voltage curve profile is directly proportional indicates the acceleration of the car. The voltage was increased from 0V to 36V and then remains at voltage at 36 V constantly. This is because the voltage is directly proportional to the velocity of the car. Acceleration performance can be determined by looking at acceleration time. This value represents linear and angular acceleration of the car. While, constant velocity on the graph represents a combination of aerodynamic resistance and rolling resistance. These values can be used to calibrate the test bench later.

The formulation used to simulate actual vehicles acceleration on the test bench is based on kinetic energy. This was done by comparing kinetic energy of the flywheel and the car. As is known, the general formula of kinetic energy,  $E_k$  of moving car are as following equation;

$$E_k = \frac{1}{2} m_c v^2 + \frac{1}{2} \omega_c^2 I_c \tag{13}$$

where  $m_c$  represents car mass,  $v$  represents car velocity,  $\omega_c$  represents car wheels angular velocity and  $I_c$  represents total car wheels moment of inertia. The formula for kinetic energy of the static rotating flywheel is as the following equation;

$$E_k = \frac{1}{2} \omega_{fw}^2 I_{fw} \tag{14}$$

where  $\omega_{fw}$  represents flywheel angular velocity and  $I_{fw}$  represents total flywheel moment of inertia. Both equations are then to be equated for the purpose of finding the required mass flywheel as follows;

$$I_{fw} = \frac{m_c v^2 + \omega_c^2 I_c}{\omega_{fw}^2} \tag{15}$$

**Simulating aerodynamic resistance component**

Car aerodynamic resistance is emulated by use concept of a Rushton turbine. By using the general formula of aerodynamic force, both elements were equated according to the equation below.

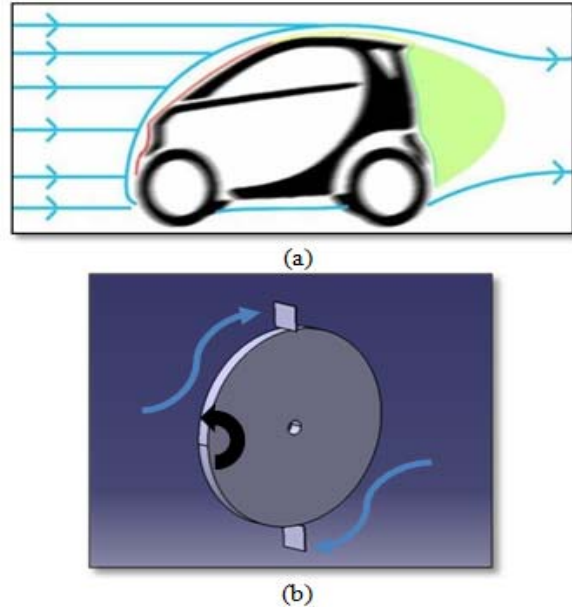


**Figure-4.** Flow stream of (a) car (b) rotating flywheel with ‘Rushton’ turbine blade.

$$F_{ad} = \frac{1}{2} \rho A_c v_c^2 C d_c = 2 \left( \frac{1}{2} \rho A_b v_b^2 C d_b \right) \tag{16}$$

$$A_b = \frac{A_c v_c^2 C d_c}{v_b^2 C d_b} \tag{17}$$

The drag coefficient of blades was determined. The experiment was conducted to test the power consumed by the electric motor of different blade sizes. The experiments were carried out in two instances with velocities of 17km/h and 26km/h. Testing was repeated five times to get more effectively average value. The results are shown in the Figure-5 below;

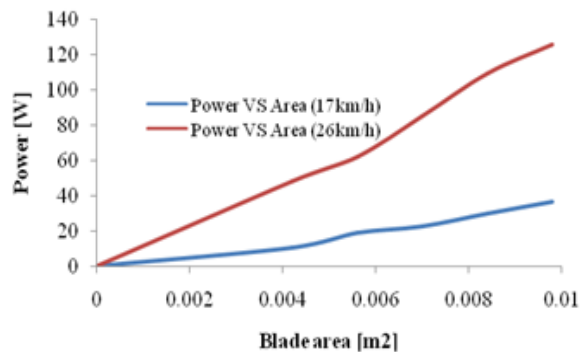


**Figure-5.** Power consumed by motor versus blade area.



**Simulating rolling resistance component**

The test bench using only one wheel to represent the four wheels of the car. The easiest way to determine the rolling resistance of one wheel is by dividing the rolling resistance of a car with four. Therefore, the calculation is:

$$F_{rr} = \frac{mgC_{rr}}{4} \tag{18}$$

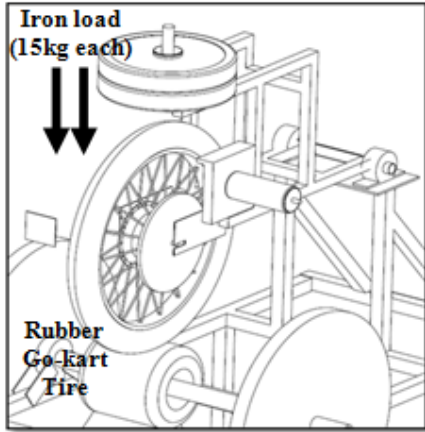


**Figure-6.** Shows the load placed on top of wheel to perform appropriate rolling resistance of actual car.

However, the distribution of rolling resistance force at each wheel cannot be made equally because the centre of gravity ratio between front and rear wheels is about 40:60. This ratio is obtained by putting the car on a standing weighing scale at each wheel. The reason we cannot take into account the rolling resistance force acting on wheel using a formulation is because of different road surfaces and test bench roller surface. According to the

literature review, the coefficient of rolling resistance for ‘Michelin Radial’ tires used is 0.025 when operating on asphalt concrete road [6]. But on the test bench, we used go-kart wheels and tires as the simulated road surface as per Figure-6. Therefore, this numerical technique for determining the test bench rolling resistance is not accurate. So, we measured the car load and calibrated the test bench by putting the load down one by one until the reading of the test bench showed the true power of the car. Figure-7 shows an experimental result of load variation versus power consumed by motor. This experiment was done by ensuring both tire pressures were 3 bars.

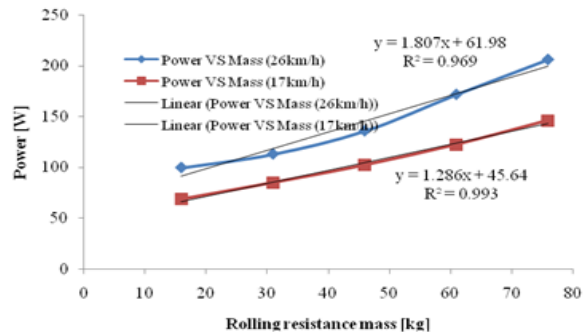


**Figure-7.** Shows a power required for every 15kg mass placed above the wheel.

**RESULTS AND DISCUSSIONS**

**Test bench calibration**

The equivalent values resulting from the analysis of each acceleration load, aerodynamic resistance load and rolling resistance load are shown in the following table.

**Table-2.** The equivalent relationship between actual car loads and simulated test bench loads.

Car		Test bench	
Component	Related Element	Component	Related Element
Acceleration	170kg total mass + 0.6743kg/m <sup>3</sup> wheels inertia	Acceleration	0.02326kg/m <sup>3</sup> drum inertia + 2.8586kg/m <sup>3</sup> flywheels inertia
Aerodynamic resistance	0.27 drag coefficient and 0.93m <sup>2</sup> frontal area	Aerodynamic resistance	4.3 drag coefficient and 0.0049m <sup>2</sup> frontal area
Rolling resistance	170kg total mass	Rolling resistance	25kg iron + 12kg traction wheel + 16kg structure

The test bench was calibrated by comparing three methods of acceleration analysis. As in the Figure-8 below, the blue coloured line shows the results of mathematical modelling; red coloured lines show the results of a test bench; and green coloured lines show the results of on-road testing. From these three tests, it was found that the profile of these accelerations curve respectively show almost similar profile. Therefore, it can

be concluded that the artificial loads to simulate real loads from the vehicle was successfully made.

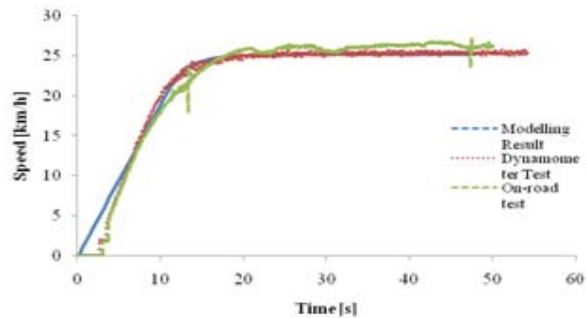


**Figure-8.** 30 A acceleration profile for three different testing of mathematical modelling, test bench experimental and actual on-road test.

## CONCLUSIONS

A series of modeling's and experiments were performed to identify the performance of three different acceleration profiles in developing inertia dynamometer for UiTM prototype fuel cell electric vehicle. The first profile was the actual acceleration of the car measured in actual road tests. The second profile was the modeled acceleration using actual values of the vehicle parameter and electric motor parameter. The third profile was the acceleration of inertia dynamometer. Comparisons were made between these three acceleration profiles and the results show a positive comparison between them. We can conclude that our methodology of designing and calibrating the inertia dynamometer was performed. This dynamometer can be a great tool to study the development of efficient electric power train system because it has capability to evaluate dynamic torque, speed and efficiency thus useful to improve the performance of vehicle.

## ACKNOWLEDGEMENTS

The authors gratefully acknowledge the financial support given for this work by the Universiti Teknologi MARA under the Tabung Amanah HEP and Tabung Amanah Pembangunan Akademik HEA in the year of 2012 for this research development and also MOE FRGS grant (600-RMI/FRGS 5/3 (54/2012)) for supporting this manuscript. Thousands of thanks to all UiTM Eco Planet team members that have led to the construction of UiTM FCEV.

## REFERENCES

- [1] K. Bhaskar, G. Nagarajan and S. Sampath. 2010. Experimental investigation on cold start emissions using electrically heated catalyst in a spark ignition engine. *International Journal of Automotive and Mechanical Engineering*. Vol. 2, pp. 105-118.
- [2] M.S. Rahmat, F. Ahmad, A.K. Mat Yamin, V.R. Aparow and N. Tamaldin. 2013. Modeling and torque tracking control of permanent magnet synchronous motor (PMSM) for hybrid electric vehicle. *International Journal of Automotive and Mechanical Engineering*. Vol. 7, pp. 955-967.
- [3] I. Salleh, M.Z. Md. Zain and R.I. Raja Hamzah. 2013. Evaluation of annoyance and suitability of a back-up warning sound for electric vehicles. *International Journal of Automotive and Mechanical Engineering*. Vol. 8, pp. 1267-1277.
- [4] M. Kamil, M.M. Rahman and R.A. Bakar. 2011. Performance evaluation of external mixture formation strategy in hydrogen fueled engine. *Journal of Mechanical Engineering and Sciences*. Vol. 1, pp. 87-98.
- [5] M. Kamil, M.M. Rahman and R.A. Bakar. 2013. Integrated simulation model for composition and properties of gases in hydrogen fueled engine. *International Journal of Automotive and Mechanical Engineering*. 8: 1242-1155.
- [6] W.A.N.W. Mohamed and R. Atan. 2012. Polymer electrolyte membrane fuel cell. *International Journal of Automotive and Mechanical Engineering*. Vol. 5, pp. 648-659.
- [7] J. Koebler. 2013. Hyundai becomes first company to mass produce hydrogen fuel cell cars, in, U.S. News, New York.
- [8] T.J. Times. 2014. Toyota to go hydrogen in December, in, The Japan Times, Nagoya.
- [9] L. James and L. John. 2003. *Electric vehicle technology explained*, Wiley.
- [10] P. Wolm, X. Chen, J.G. Chase and W. Pettigrew. 2010. Analysis of a PM DC motor model for application in feedback design for electric-powered mobility vehicles. *International Journal of Computer Applications in Technology*. Vol. 39, pp. 116-122.
- [11] L.S. Sundar, M.H. Farooky, S.N. Sarada and I.C.H.M. M K Singh. 2013. Experimental thermal conductivity of ethylene glycol and water mixture based low volume concentration of Al<sub>2</sub>O<sub>3</sub> and CuO nanofluids. *International Communications in Heat and Mass Transfer*. Vol. 41, pp. 41-46.
- [12] H. Zhang, Q. Wu, J. Lin, J. Chen, Z.X.A.P. 124304. 2010. Thermal conductivity of polyethylene glycol nanofluids containing carbon coated metal nanoparticles. *J. Appl. Phys.* Vol. 108, pp. 124304-124309.
- [13] R. Manning, Ewing and J. (2009). *RACQ Vehicles Technologies. Temperatures in cars survey*. RACQ Vehicles Technologies. pp. 1-21.



- [14] J. Papuga. 2011. A survey on evaluating the fatigue limit under multiaxial loading. *International Journal of Fatigue*. Vol. 33, pp. 153-165.
- [15] G. Wasselynck, B. Auvity, J.-C. Olivier, D. Trichet, C. Josset, P. Maindrin. 2012. Design and testing of a fuel cell powertrain with energy constraints, *Energy*. Vol. 38, pp. 414-424.
- [16] J. Wang, M.-X. Lu, L. Zhang, W. Chang, L.-N. Xu, L.-H. Hu. 2012. Effect of welding process on the microstructure and properties of dissimilar weld joints between low alloy and duplex stainless steel. *International Journal of Minerals, Metallurgy and Materials*. Vol. 19, pp. 518-524.
- [17] M.M.Noor, A.P. Wandel and Talal Yusaf. 2014, Simulation of biogas combustion in MILD burner. *Journal of Mechanical Engineering and Sciences*. pp. 995-1013.